Aqueous synthesis of CdTe quantum dot as biological fluorescent probe for monitoring methyl parathion by fluoro-immunosensor

RAGHURAJ S. CHOUHAN, AAYDHA C. VINAYAKA AND MUNNA S. THAKUR*

Fermentation Technology & Bioengineering Department

Central Food Technological Research Institute (A constituent laboratory of Council of Scientific and Industrial Research, New Delhi), Mysore-570020, India

*** Corresponding author**

M.S. Thakur, Ph.D.

Senior scientist

Fermentation technology & Bioengineering Department

Central Food Technological Research Institute, Mysore-570020, India

msthakur@cftri.res.in, msthakur@yahoo.com

Bioconjugation of quantum dots (QDs) provide high resolution in biological fluorescent labelling as a result of physical and optical properties of QDs. This intrinsic property of QDs can be made use of for sensitive detection of target analytes including food and environmental monitoring. In this investigation, we report the bioconjugation of thiol stabilized CdTe QD for the sensitive detection of methyl parathion (MP) at picogram level. The specificity in the analysis was attributed by highly specific competitive immunological reactions between free MP and CdTe QD bioconjugated MP (MP-BSA-CdTe) for immobilized anti-MP IgY antibodies in a simple flow injection system. We also report the possible resonance energy transfer phenomenon as a result of nanobiomolecular interaction obtained through the bioconjugation of CdTe QD with protein bovine serum albumin (BSA). This has resulted in a significant change in the photo-absorption of CdTe QD, which can be made use for future nanosensor development.

Quantum dots (QDs) are semiconductor nanoparticals (NPs), which have gained a lot of interest in the biological research areas because of their unique spectral properties.[1, 2] These smart NPs are made up of II-VI, III-V and IV-VI group elements of the periodic table.[3] The long photostability, broad absorption and narrow emission properties of these molecules have made them superior to conventional organic fluorescent dyes. Moreover, water soluble QDs have proved to be the choice of interest in biological labelling due to their biocompatibility.[4, 5] As a result, these NPs are being used in various areas of biological research such as targeted drug delivery system, cellular labelling, to detect site directed mutagenesis and molecular therapeutics.[6-9] The intrinsic narrow emission property of these QDs can also be used for the environmental monitoring including sensitive detection of targeted analytes. The bioconjugation of QDs with biomolecules such as protein based haptens and immunoglobulin provides a way to achieve the specificity and high sensitivity aimed at the targeted analyte detection. The hybrid materials obtained through the bioconjugation of QDs with proteins also provides an insight into the study of energy transfer phenomenon.[10] The possibility of obtaining resonance energy transfer in bioconjugated CdTe QD and CdSe QD were well established in previous reports.[10-12] The spectral overlap of donor and acceptor chromophores resulting as a consequence of bioconjugation between CdTe QD and proteins may be exploited by monitoring the photo-absorption spectra of these hybrid molecules.[10] The energy transfer processes as a result of bioconjugation can

also be utilized in future nanosensor developments aimed at the sensitivity and specificity in multiplexed analyte detections.

Green revolution has resulted in increased agricultural productivity that was made possible with the use of various organic formulations such as pesticides and fertilizers.[13] Pesticides are being used world wide to combat the destructive effects caused by pests and insects in agriculture, food storage facilities and even in public health operations.[14] MP being an organophosphorous class of pesticide is extensively being used to prevent crop loss caused by stem borer, grey weevil, brown plant hoppers in the field of sugarcane, rice , apple, grape, mango plantation in various parts of the world.[15-17] The enormous use of MP has lead to the significant ground water contamination, which has depicted in various food formulations, drinking waters and in food chain.[18,19] Consequent health related hazardous effects caused by the potential exposure of moderate to higher levels of MP can generate toxicological risks such as itching, skin irritation, stomach cramps, epigastria, abdominal pain, chest tightness, productive cough, dyspnoea and basal crepitating of both lungs. Previous reports of certain haematological diseases such as significant decrease in haemoglobin count, decreased size of red blood cells (RBCs), and impairment in heme biosynthesis,[16] realises the importance of addressing the MP contamination.

Previously reported assay techniques for the detection of MP based on electrochemical and optical detection systems, [20, 21] have significant limitations. An inadequate sensitivity and the difficulties associated with the dissociation of pesticide from the immobilized enzyme have become obstacle for the

development of enzyme-based biosensor for OP pesticides. The limitations associated with the conventional analytical techniques such as gas chromatography, [22] liquid chromatography, [23] and ELISA [24] in terms of cost effectiveness, sample pre-treatment, skilled personnel and analysis time have opened up an opportunity for the development of newer techniques with increased merits.

Therefore, present investigation reports the integration of high specificity of immunological reactions with magnetic and optical behavior of CdTe QDs to develop a nanobiosensor for the sensitive monitoring of environmental pollutants and toxicants such as pesticides considering MP for the case study.

Aqueous synthesis of CdTe Quantum dots

CdTe QD was synthesized by aqueous method according to the method described.[3] Aqueous method has allowed attaining biocompatibility in the synthesized QDs, which was the primary criterion for obtaining water soluble QDs.[25] Mercaptopropionic acid has stabilized the QD along with providing functional carboxylic group necessary for further bioconjugation in aqueous medium. Transmission electron microscopic studies (TEM) on thus synthesized CdTe QD have indicated the narrow particle size distribution in the aqueous medium. On average, the particle size of CdTe QD was determined to be 3 ± 0.5 nm (Figure 1, right image) with well dispersed in the aqueous medium.[25] The results over particle size of CdTe QD thus obtained by TEM was well supported

by Atomic Force Microscopy (AFM, Figure 1, left image). A well defined broad photo-absorption spectrum and narrow emission spectrum at 551-553 nm with full width at half maximum (FWHM) of 65 nm - 69 nm has confirmed the synthesis of homogenous CdTe QD. CdTe QDs thus synthesized were covalently bioconjugated with MP to obtain the bioconjugate in presence of BSA as a biological linker.

CdTe QD was analyzed by TEM at 200 KV using 400 mesh carbon copper grid from pacific grid technology. CdTe QDs of 3 ± 0.5 nm was observed to be well dispersed in the aqueous medium which has shown photoemission at 550 nm with full width at half maximum (FWHM) of 65 nm - 69 nm.

Bioconjugation of MP-hapten

MP being low molecular weight compound (263.21 g/mol), is non-immunogenic in nature; therefore, it was found essential to bioconjugate with a suitable protein molecule to render immunogenicity without altering its epitope. BSA was used as a carrier molecule and bioconjugated successfully to make MP-BSA immunogenic, which was determined to be relatively resistant to denaturation. During MP hapten synthesis, the primary amino terminal of O-4-aminophenyl O, O dimethyl phosphorothioate positioned at 4^{th} carbon was derivatized to obtain 4-(4-(dimethoxyphosphorothioyloxy) phenyl amino)-4-oxobutanoic acid having functional carboxylic terminal as shown in Scheme 1a (Supplementary Figure

1S). The extent of conjugation of derivatized MP with BSA was confirmed by fourier transfer infrared spectroscopy (FTIR). The presence of strong characteristic –C=O-stretch at 1703 and 1746 cm^{-1} including carboxylate absorption at 1609 cm^{-1} and $–CH_3$- stretch at 1380 cm^{-1} confirms the derivatization of MP. Later the conjugation of MP-hapten with protein BSA (Scheme 2b) was confirmed by the presence of characteristic carbonyl group absorption at 1784 cm^{-1} and characteristic strong amide absorption (–CO-NH-) at 1655 cm^{-1}. Conjugation of MP-hapten with protein BSA was further confirmed by TNBS assay by monitoring the modification of ϵ-amino groups of protein BSA with MP-hapten. The percent conjugation was restricted to 40-45% by optimizing the condition that has permitted to further bioconjugate the MP-BSA with thiol capped CdTe QD to obtain MP-BSA-CdTe (Scheme 1b).

Protein BSA was used as a biological linker during the synthesis of MP-BSA-CdTe bioconjugate that has provided stability to the bioconjugate. Circular dichroism (CD) spectra were taken for BSA and MP-BSA-CdTe bioconjugate to monitor the effects of CdTe QD on BSA in the bioconjugate (Figure 2). CD spectrum of MP-BSA-CdTe bioconjugate has revealed the stable conformation of BSA upon bioconjugation with CdTe QD nanoparticle as it was compared with standard BSA molecule.

Confirmation of bioconjugation

Both photo-absorption spectrum and gel electrophoresis have confirmed the successful bioconjugation of CdTe QD. Photo-absorption of MP-BSA-CdTe bioconjugate was taken to monitor the optical behavior of the bioconjugate that might have got influenced by CdTe QD. The photo-absorption spectrum of BSA has got changed as a result of bioconjugation with CdTe QD (Figure 3). BSA being protein has shown characteristic absorption maxima at 280 nm, which is specific for aromatic amino acids. The characteristic absorption spectrum of MP-BSA-CdTe bioconjugate was found differing from that of BSA and CdTe QD alone. CdTe QD has got broad absorption spectrum, which has shown an interesting absorption peak at 310 nm as a result of bioconjugation with BSA. Absorption of 0.644 units at 310 nm for the bioconjugate was of considerable interest as the same was absent in both standard BSA and CdTe QD alone. This confirms the successful bioconjugation of CdTe QD with BSA.

The bioconjugation was further confirmed by monitoring the mobility of MP-BSA-CdTe bioconjugate in polyacrilamide gel electrophoresis (PAGE). Both native-PAGE (Figure 4A) and sodium dodecyl sulphate (SDS) PAGE (Figure 4B) results confirmed the bioconjugation of CdTe QD to BSA. The influence of high negative charge of CdTe QD on protein BSA was observed by the mobility of MP-BSA-CdTe bioconjugate under native conditions. Theoretically, increased molecular weight would result in decreased mobility of the protein sample. In

native-PAGE, as the mobility of proteins relies upon both molecular weight and their native charge, the charge coupled interactions of CdTe QD on BSA was observed. Contrary to the mobility of standard BSA, MP-BSA-CdTe bioconjugate has shown increased mobility. The mobility of MP-BSA-CdTe bioconjugate has got increased even though there was an increase in the molecular weight of the bioconjugate.

Contrary to native-PAGE, the mobility of proteins relies upon the molecular weight differences in the SDS-PAGE. As the native charges of the protein samples being masked by SDS, which imparts a net negative charge that remained similar for all samples, the mobility of protein samples were generally not get affected by the native charges. As a result there were not any considerable differences in the mobility of bioconjugated and standard BSA samples as it was observed in Figure 4B. Moreover, the presence of observable luminescence as it was shown by UV illumination for MP-BSA-CdTe sample (Figure 4C, lane 3) further confirmed the covalent conjugation of CdTe QD. Contrary to standard CdTe QD (lane 4), the bioconjugated CdTe QD has not moved apart considerably but stayed with protein BSA revealing stable strong covalent bond among them. Further MP-BSA-CdTe bioconjugate was made use for the sensitive detection of MP by fluoroimmunoassay technique.

Competitive fluoroimmunoassay

The fluoroimmunoassay technique was based on the integration of highly sensitive fluorescence provided by QDs and high specificity of immunological reactions. The assay specificity was attained by the highly specific immunological reactions between MP and anti-MP IgY antibodies. Immunizing white leghorn chickens with MP-BSA has generated IgY class immunoglobulins that were later isolated from egg yolk. The MP-IgY antibodies produced in white leghorn hen eggs were tested for both protein and antibody titre. There was a substantial increase in the protein concentration with each booster injections, which will indicate the generation of immunoglobulins. Anti-MP IgY was extracted from egg yolk by water dilution method, which was preferred over other extraction procedures in order to get high yield and pure IgY antibodies with high titre values.[26, 27]

The extracted anti-MP IgY antibodies were purified by BSA affinity column to remove any anti-BSA antibodies that would have generated as a result of immunization with MP-BSA (Supplementary Figure 2S). Indirect non-competitive ELISA tested isolated antibodies for better titer values and it was observed that antibodies showed higher titer values after third and fourth booster doses. Indirect competitive ELISA showed the antibodies to be highly purified and proved more specific and sensitive after affinity purification through BSA column. SDS-PAGE has carried out for further confirmation of the purity of anti-MP IgY antibody. The presence of bands indicating heavy chain and light chains of antibodies at 62 and 42 KDa, suggests the absence of any native protein

contamination in the purified immunoglobulins samples (Supplementary Figure 3S).

Immobilization of anti-MP IgY was found to be very critical factor as the fluoroimmunoassay technique relies on specific interactions between immobilized anti-MP IgY antibody and MP pesticide in a flow through immunoreactor column. The concentration of antibodies for immobilization was optimized based on the percent binding of MP-BSA-CdTe bioconjugate (25 µL from 1:5000 dilution of 1 mg/mL concentration) to be passed through the immunoreactor column. The concentration of MP-BSA-CdTe bioconjugate to be passed through immunoreactor column was fixed based on the fluorescent intensity shown by the bioconjugate at 350 nm excitation wavelength.

During optimization, different concentrations (5, 10, 20 and 50 µg/mL) of antibodies were immobilized and optimized by passing known amount of MP-BSA-CdTe bioconjugate through the antibody immobilized immunoreactor column. Percentage binding of MP-BSA-CdTe bioconjugate was monitored based on the fluorescence shown by the bioconjugate that will come out of the column. Maximum binding of bioconjugate was observed for immobilized antibody concentration higher than 20 µg/mL of sepharose, with very low fluorescence for the bioconjugate coming out of the column). Lower concentrations of antibodies have shown lesser percentage of binding and larger amounts of MP-BSA-CdTe bioconjugate came out of the immunoreactor column giving more fluorescence. Therefore, antibodies above 20 µg concentrations were found to be in excess for immobilization. Therefore, 20 µg of antibody was

selected as an optimum concentration that had shown optimal binding required to carry out further immunosensor studies.

During competitive fluoroimmunoassay, the bioconjugate that was eluted out of the immunoreactor column was collected and further scanned for intensity of fluorescence in a fluorimeter (Supplementary Figure 4S). The elution of MP-BSA-CdTe bioconjugate depends on the concentrations of free MP passed as a result of competitive binding among them for the known concentrations of immobilized anti-MP antibodies. It was observed that the elution of MP-BSA-CdTe bioconjugate was directly proportional to the extracted MP passed in the range 1 ng/mL – 0.1 ng/mL (Figure 5). Thus, with the fluoroimmunoassay technique it was possible to detect extracted MP up to a sensitivity of 0.1 ng/mL concentration.

Discussion

Stability of the bioconjugate is a critical factor for both qualitative and quantitative bioalalytical techniques. Therefore, while confirming the stability of MP-BSA-CdTe bioconjugate, CD spectral studies were performed to monitor the 3D conformation of protein BSA in the bioconjugate. The protein in the bioconjugate was found to be intact enough to retain its tertiary and quaternary conformation. This has ruled out the drastic effects of highly negatively charged CdTe QD, which otherwise would have degraded the protein molecule. There was no spectral shift observed for MP-BSA-CdTe bioconjugate and was determined to

be well comparable to standard BSA. The stability of protein to retain its confirmation upon bioconjugation with CdTe QD, as it was revealed by CD spectra, may open up an opportunity for various applications of CdTe QDs in the biological field. Thus CD spectrum confirmed the stability of the bioconjugate.

While analyzing the photo-absorption spectra for MP bioconjugates, it was observed a peak shift of 10 nm from 280 nm to 270 nm for MP-BSA and a characteristic absorption peak at 320 nm for MP-BSA-CdTe bioconjugate. The shift in the absorption maximum from 280 nm to 270 nm was a characteristic feature of the presence of aminophenolic group in 4-(4-(dimethoxyphosphorothioyloxy) phenyl amino)-4-oxobutanoic acid, which was the derivatised version of the MP (Supplementary Figure 1S). As such, there was no significant absorption for MP-BSA and standard CdTe QD in the range of 310 nm to 320 nm that has appeared as a result of bioconjugation with CdTe QD. The new absorption peak observed at 310 nm might be due to the interactions of CdTe QD with protein BSA in the MP-BSA-CdTe bioconjugate. The protein BSA might have undergone a slight conformational change that has lead to the overall structural and dimensional change in the bioconjugate. Absorption peak in the range of 310 nm to 320 nm was due to the covalent conjugation of CdTe QD and MP-BSA. Covalent conjugation has resulted in optical interactions between CdTe QD and BSA which could be the possible resonance energy transfer among them. The possibility of having resonance energy transfer between NPs and biomolecules were previously been reported.[10, 11] The spectral overlap between donor and acceptor chromophores, which is the primary requirement for

energy transfer phenomenon, was attained in MP-BSA-CdTe bioconjugate by covalent conjugation. BSA being protein in nature has its emission maximum in the range of 310 nm to 340 nm, as a result of aromatic amino acids such as tyrosine, tryptophan and phenyl alanine. Because of the broad absorption spectrum of CdTe QD, spectral overlap is possible between BSA as an energy donor and CdTe QD as an energy acceptor in the bioconjugate. Thus, covalent conjugation between BSA and CdTe QD has brought the two chromophores to such close proximity in the MP-BSA-CdTe bioconjugate. Therefore, excitonic energy of protein BSA might have got transferred to CdTe QD in the bioconjugate resembling foster resonance energy transfer (FRET) phenomenon. Thus, the bioconjugation was confirmed by absorption spectral analysis of MP-BSA-CdTe bioconjugate. Furthermore, our experiment on the mobility of MP-BSA-CdTe bioconjugate in gel electrophoresis has revealed the dominance of charge over the molecular weight as a result of bioconjugation. This could be due to the over all structural compactness of the bioconjugate and the high negative charge of CdTe QD that might have compensated the increased molecular weight providing a net negative charge to the bioconjugate. The shift in the band position of BSA monomer makes it evident that CdTe QD has got covalently bioconjugated resulting in high negativity to the bioconjugated BSA molecule. The appearance of two other bands above the characteristic BSA monomer band could be due to the presence of BSA-BSA dimer and globulins respectively in the commercial sample. [28]

In our present fluoroimmunoassay technique, using IgY over IgG was found advantageous in terms of avoiding bleeding of the animal, isolation of antibodies were determined to be simple and less quantity of antigen required to obtained specific IgY with high titer. Moreover, the yield of IgY antibody was approximately 100 mg/egg yolk without any IgA or IgM contamination. The possibility of getting IgA and IgM in the egg yolk was very low as both IgA and IgM were transferred from oviduct into the egg white together with other proteins. On the other hand the transfer of IgY in the egg follicle was receptor mediated and therefore they were reportedly present in egg yolk in large quantities.[26, 27] In proposed fluoroimmunoassay technique, competitive binding between extracted MP and known concentration of MP-BSA-CdTe bioconjugate for immobilized anti-MP IgY antibody has detected the concentration of extracted MP from spiked juice and water samples. As the concentration of immobilized antibody remains constant in the immunoreactor column, the variation in the concentration of extracted MP will affect the binding of MP-BSA-CdTe bioconjugate and its elution from the immunoreactor column (Supplementary Figure 4S). Here the binding of MP-BSA-CdTe bioconjugate was depended on the left over antibody after the binding of extracted MP in the immunoreactor column. Higher the extracted MP concentration, lower will be the binding of MP-BSA-CdTe bioconjugate and the bioconjugate coming out of the column will be more which gives maximum fluorescence signals. Therefore, the appropriate concentration of antibody for immobilization was found to be very critical factor.

In brief, quantitative determination of MP was accomplished by competitive fluoroimmunoassay principle at a high sensitivity level (0.1 ng/mL). This technique offers several advantages over standard HPLC, GC and ELISA methods as proposed method is based on antigen - antibody reaction along with highly fluorescent CdTe QD which makes highly sensitive and specific detection to the pesticide of interest (MP). The results obtained in the present studies are expected to lead to the development of a rapid, reliable and field applicable biosensor with high sensitivity (pg level). Application of IgY in analytical and in-vitro studies is advantageous compared to IgG in terms of its stability, high antibody production capacity and cost effectiveness. The present method based on NPs is quite promising and has the potential application for other class of different pesticide and toxins.

Acknowledgement.

The authors thank the Director, CFTRI, Mysore, for providing facilities. Mr. R.S. Chouhan is thankful to Council of Scientific and Industrial Research (CSIR) for Senior Research Fellowship. Department of Biotechnology, Government of India and Swiss Development Cooperation, Switzerland to provide financial support under Indo-Swiss Biotechnology collaborative project gratefully acknowledged. Dr. K.R. Thampi, Dr. Sridevi A. Singh, Dr. P. Srinivas, Dr. K. N. Gurudutt and Dr. Sanjukta Patra, IIT, Gowahati are acknowledged for there kind help and support.

References

1. Ramadurai, D. *et al*. Electrical and optical properties of colloidal semiconductor nanocrystals in aqueous environments. *Superlat. Microstruct.* **40**, 38–44 (2006).
2. Pathak, S., Davidson, M. C. & Silva, G. A. Characterization of the functional binding properties of antibody bioconjugated quantum dots. *Nano. Lett.* **7**, 1839-1845 (2007)
3. Bao, H., Gong, Y., Li, Z. & Gao, M. Enhancement effect of illumination on the photoluminescence of water soluble CdTe nanocrystals: Towards highly fluorescent CdTe/CDs core shell. *Struct.. Chem. Mater*. **16,** 3853-3859 (2004).
4. Bruchez, M. Jr., Moronne, M., Weiss, G. P. S. & Alivisatos, A. P. Semiconductor nanocrystals as fluorescent biological labels. *Science* **281,** 2013-2016 (1998).
5. Weng, J. F. *et al*. Highly luminescent CdTe quantum dots prepared in aquous phase as an alternative fluorescent probe for cell imaging. *Talanta* **70,** 397-402 (2006).
6. Csaki, A., Maubach, G., Born, D., Reichart, J. & Fritzsche, W. DNA based Molecular Nanotechnology. *Single Mol.* **3,** 275-280 (2002).
7. Ho, Y. P., Kung, M. C., Yang, S. & Wang, T.H. Multiplexed hybridization detection with multicolour colocalization of quantum dot nanoprobes. *Nano Lett.* **5,** 1693-1697 (2005).

8. Bakalova, R. *et al*. Quantum dot anti-CD bioconjugate: Are They Potential Photostabilizers or potentiators of Classical photosensitizing Agents in Photodynamic Therapy of Cancer. *Nano Lett.* **4,** 1567-1573 (2004).
9. Yen, H. C., Ho, Y. P., Shin, L.M. & Wang, T.H. Homogeneous point mutation detection by quantum dot-mediated two color fluorescence coincidence analysis. *Nucleic. Acid Research.* **34,** 1-8 (2006).
10. Vinayaka, A. C., Basheer, S. & Thakur, M. S. Bioconjugation of CdTe quantum dot for the detection of 2,4-Dichlorophenoxyacetic acid by competitive fluoroimmunoassay based biosensor. *Biosens. and Bioelectron.*, **24,** 1615-1620 (2009).
11. Mamedova, N. N., Kotov, N. A., Rogach, A. L. & Studer, J. Albumin-CdTe nanoparticle bioconjugates: preparation, structure and interunit energy transfer with antenna effect. *Nano Lett.* **1,** 281-286 (2001).
12. Ma, Q. *et al.* Fluorescence resonance energy transfer in double-quantum dot labelled IgG system. *Talanta* **67,** 1029-1034 (2005).
13. Fox, J. E., Gulledge, J., Engelhaupt, E., Burow, M.E. & Mclachlan, J.A. Pesticides reduce symbiotic efficiency of nitrogen fixing rhizobia and host plants. *PNAS* **104,** 10282-10287 (2007).
14. US EPA, Summary of the Risks and Uses of organophosphate Methylparathion,2000.http://www.epa.gov./pesticides/op/methyl_parathion/methylsum.htm.

15. Rastogi, S. K. *et al.* Monitoring of plasma butyrylcholinesterase activity and haematological parameters in pesticides sprayers. *Ind. J. Occup. Environ. Medi.* **12,** 29-32 (2008)
16. Oliva, J., Barba, A., Vela, N., Melendreras, F. & Navarro, S. J. Multiresidue method for the rapid determination of organophosphorus insecticides in grapes must and wine. *Chromatography A*. **882,** 213-220 (2000).
17. Pappas, C. J., Kyriakidis, N. B. & Athanasopoulos, P. E. Degradation of parathion methyl on field-sprayed apples and stored apples. *J. AOAC*. **82,** 359-363 (1998).
18. Thakur, M. S. & Karanth, N. G. *Advances in Biosensors* (Elsevier: Amsterdam, 2003).
19. Chapalamadugu, S. & Chaudhry, G. R. Microbiological and biotechnological aspects of metabolism of carbamates and organophosphates. *Crit. Rev. Biotechnol.* **12,** 357-389 (1992).
20. Kroger, S., Setford S. J. & Turner, A. P. F. Immunosensor for 2,4 dichlorophenoxy acetic acid in aqueous organic solvent soil extract. *Anal. Chem.* **70,** 5047-5053 (1998).
21. Plowman, T. E. *et al.* Multiple analyte fluoroimmunoassay using an integrated optical waveguide sensor. *Anal. Chem.* **71,** 4344-4352 (1999).
22. Shanker, A., Sood, C., Kumar, V. & Ravindranath, S. D. A. Modified extraction and cleanup procedure for the detection and determination of parathion methyl and chlorpyrifos residues in tea. *Pest. Manag. Sci.* **57**, 458-462 (2001).

23. Galeano-Diaz, T., Guiberteau-Cabanillas, A., Mora-Diez, N., Parrilla-Vazquez, P. & Salinas-Lopez, F. Rapid and sensitive determination of 4-nitrophenol, 3-methyl-4-nitrophenol, 4,6-dinitro-o-cresol, parathion methyl, fenitrothion and parathion ethyl by liquid chromatography with electrochemical detection. *J. Agric. Food. Chem.* **48,** 4508-4513 (2000).
24. Kim, M. J., Lee, H. S., Chung, D.H. & Lee, Y. T. Synthesis of haptens of organophosphorous pesticides and development of enzyme-linked immunosorbent assay for parathion-methyl. *Anal. Chimi. Acta.* **493,** 47-62 (2003a)
25. Li, M. *et al.* Hydrothermal synthesis of highly luminescent CdTe quantum dots by adjusting precursors concentration and their conjugation with BSA as biological fluorescent probes. *Talanta* **72,** 89-94 (2007).
26. Akita, E. M. & Nakai, S. Comparison of four purification methods for the production of immunoglobulins from eggs laid by hens immunized with enterotoxigenic E.coli strain. *J. Immunol. Meth.* **160,** 207-214 (1993).
27. Akita, E. M. & Li-Chan E. C. Y. Isolation of bovine immunoglobulin G subclasses from milk, colostrums and whey using immobilized egg yolk antibodies. *J. Dairy Sci*. **81,** 54-63 (1998).
28. Wang, S., Mamedova, N., Kotov, N. A., Chen, W. & Studer, J. Antigen/Antibody immunocomplex from CdTe nanoparticle Bioconjugates. *Nano. Lett*. **2,** 817-822 (2002).

Figure legends

Scheme 1 (a & b). Schematic representation of MP-hapten synthesis. a) Reaction of *O*-4 aminophenyl *O,O*–dimethyl phosphorothioate with dihyrofuran-2,5-dione in the presence of dry dioxane yielding 4-(4-(dimethoxyphosphorothioyloxy) phenyl amino)-4-oxobutanoic acid for the further conjugation with protein.

b) Synthjesis of MP-BSA bioconjugate by carbodiimide method in presence of *N*-hydroxy succinimide (NHS) and N- (3-dimethylaminopropyl)-N-ethylcarbodiimide hydrochloride (EDC).

Figure 1. Atomic Force Microscopy (AFM, Left) and Transmission Electron microscopy (TEM, Right) images of CdTe QD synthesized in aqueous medium. AFM picture was scanned over an area of 5 x 5 μm in tapping mode using molecular imaging system. The resonant oscillation frequency of probe was 190 – 300 KHz.

Figure 2. Circular dichroism (CD) spectra showing the intact nature of protein BSA even after bioconjugation with CdTe. The spectra for MP-BSA-CdTe QD was observed to be well coinciding with Std BSA indicating the intact 3D conformation of protein BSA.

Figure 3. Photo-absorption spectra of standard and bioconjugates. The spectral change observed for MP-BSA-CdTe bioconjugate revealing the nanobiomolecular interaction as a result of covalent conjugation.

Figure 4. Gel-electrophoresis showing the mobility of Standard and bioconjugated CdTe QD. (A) Native-PAGE stained by silver staining. (B) SDS-PAGE stained by coomassie blue R-250. (C) UV illuminated image of SDS-PAGE before staining excited at 366 nm. Lane 1 Std BSA, Lane 2 MP-BSA, Lane 3 MP-BSA-CdTe, Lane 4 Std CdTe QD.

Figure 5. Fluorescence spectra of MP-BSA-CdTe bioconjugate proportional to various concentrations of free MP passed through the immunoreactor column. The linearity was in the range of 1 ng/mL to 0.1 ng/mL.

Scheme 1.

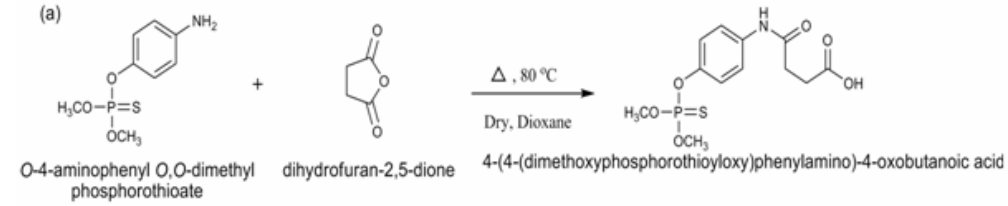

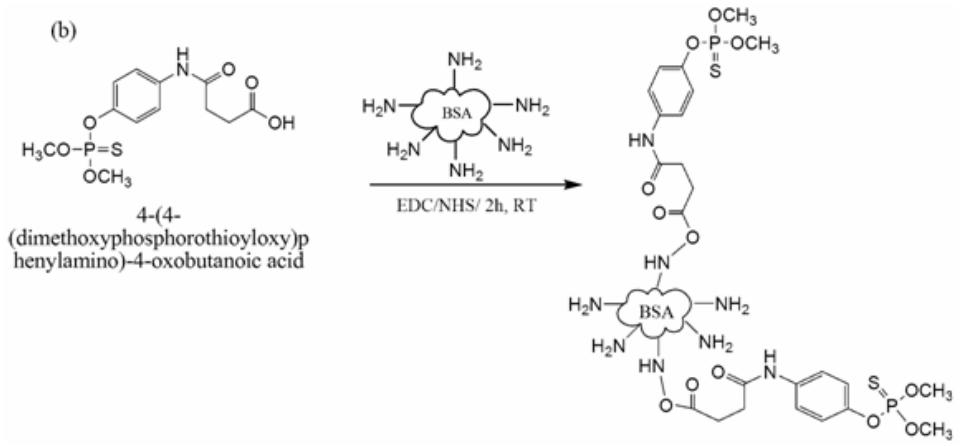

Figure 1.

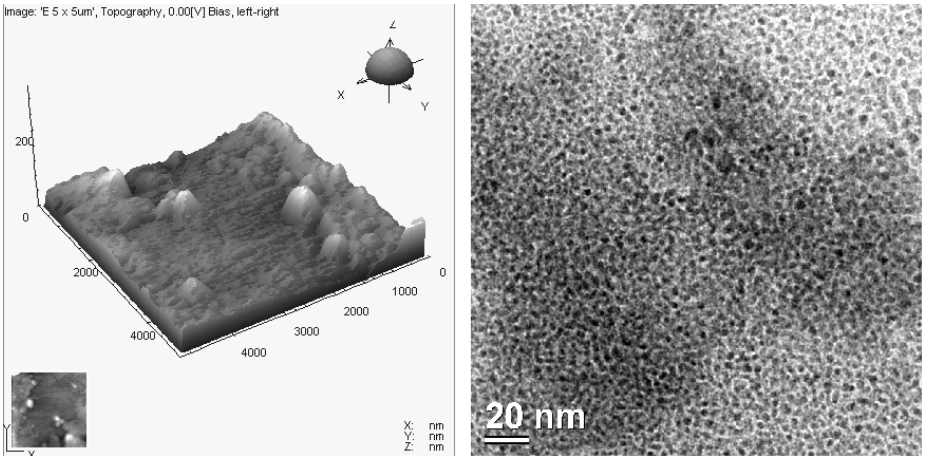

Figure 2.

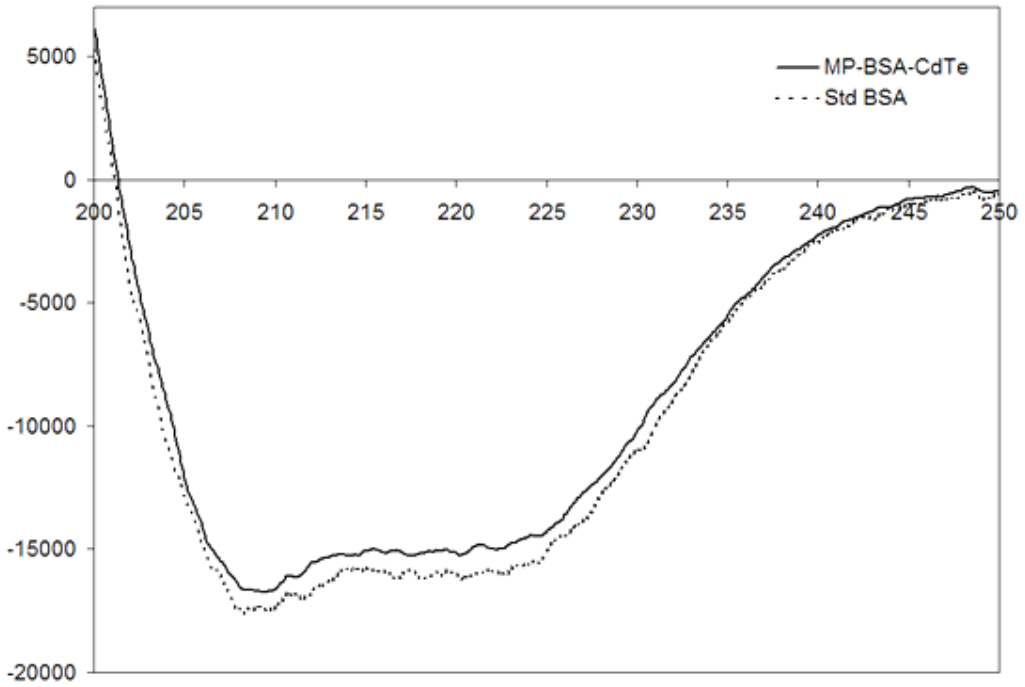

Figure 3.

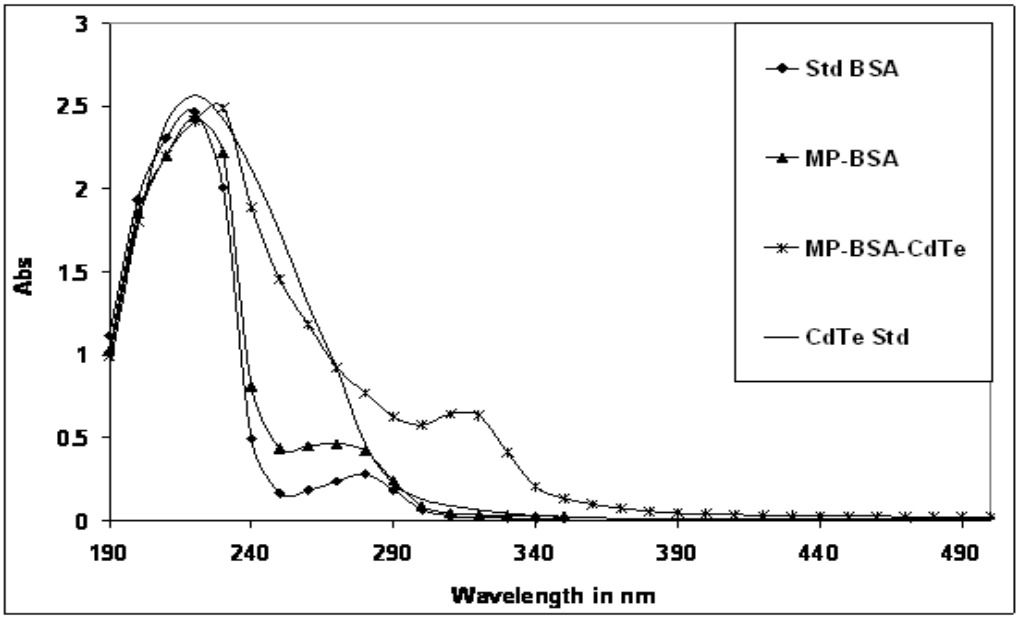

Figure 4.

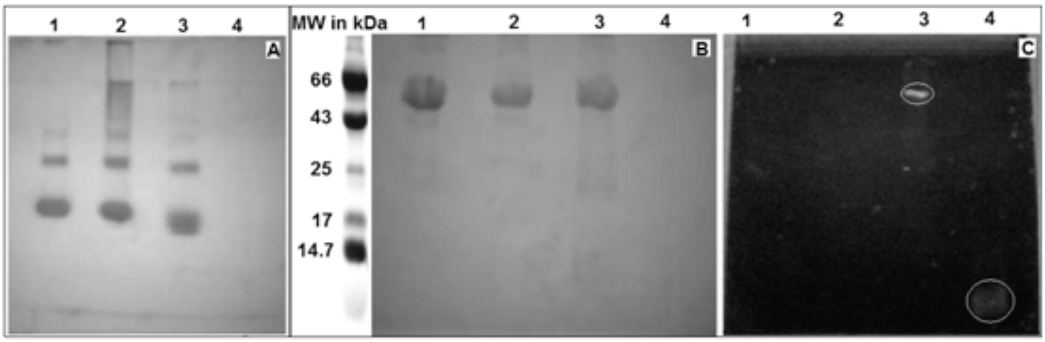

Figure 5.